electronics

Article

Adaptive Spectrum Anti-Jamming in UAV-Enabled Air-to-Ground Networks: A Bimatrix Stackelberg Game Approach

Longbo Cheng [1,2], Zixuan Xu [1,2,*], Jianshan Zhou [1,2], Daxin Tian [1,2], Xuting Duan [1,2], Kaige Qu [3] and Dezong Zhao [4]

[1] Key Laboratory of Technology on Intelligent Transportation Systems, Ministry of Science and Technology, Beijing 100088, China; chenglb@buaa.edu.cn (L.C.)
[2] School of Transportation Science and Engineering, Beihang University, Beijing 100191, China
[3] The Electrical and Computer Engineering Department, University of Waterloo, Waterloo, ON N2L 3G1, Canada
[4] School of James Watt Engineering, University of Glasgow, Glasgow G12 8QQ, UK
* Correspondence: xuzixuan@buaa.edu.cn

Abstract: Anti-jamming communication technology is one of the most critical technologies for establishing secure and reliable communication between unmanned aerial vehicles (UAVs) and ground units. The current research on anti-jamming technology focuses primarily on the power and spatial domains and does not target the issue of intelligent jammer attacks on communication channels. We propose a game-theoretical center frequency selection method for UAV-enabled air-to-ground (A2G) networks to address this challenge. Specifically, we model the central frequency selection problem as a Stackelberg game between the UAV and the jammer, where the UAV is the leader and the jammer is the follower. We develop a formal matrix structure for characterizing the payoff of the UAV and the jammer and theoretically prove that the mixed Nash equilibrium of such a bimatrix Stackelberg game is equivalent to the optimal solution of a linear programming model. Then, we propose an efficient game algorithm via linear programming. Building on this foundation, we champion an efficacious algorithm, underpinned by our novel linear programming solution paradigm, ensuring computational feasibility with polynomial time complexity. Simulation experiments show that our game-theoretical approach can achieve Nash equilibrium and outperform traditional schemes, including the Frequency-Hopping Spread Spectrum (FHSS) and the Random Selection (RS) schemes, in terms of higher payoff and better stability.

Keywords: air-to-ground network; unmanned aerial vehicle (UAV); anti-jamming communication; Stackelberg game

check for updates

Citation: Cheng, L.; Xu, Z.; Zhou, J.; Tian, D.; Duan, X.; Qu, K.; Zhao, D. Adaptive Spectrum Anti-Jamming in UAV-Enabled Air-to-Ground Networks: A Bimatrix Stackelberg Game Approach. *Electronics* **2023**, *12*, 4344. https://doi.org/10.3390/electronics12204344

Academic Editor: Mahmut Reyhanoglu

Received: 6 September 2023
Revised: 6 October 2023
Accepted: 18 October 2023
Published: 19 October 2023

Copyright: © 2023 by the authors. Licensee MDPI, Basel, Switzerland. This article is an open access article distributed under the terms and conditions of the Creative Commons Attribution (CC BY) license (https://creativecommons.org/licenses/by/4.0/).

1. Introduction

Physical-layer security is of utmost importance in unmanned aerial vehicle (UAV)-enabled communication networks. Nevertheless, UAV-enabled air-to-ground communication networks are susceptible to various malicious attacks. Spectrum jamming is particularly concerning and may result in wireless interference with unmanned aerial vehicles (UAVs), disrupting authentic data transmissions. Commonly used approaches to mitigate spectrum jamming, including frequency hopping and random selection techniques, depend on carrier frequency adaptation. Nonetheless, sophisticated spectrum sensing and learning techniques enable jammers to detect changing frequency patterns and make more effective jamming decisions. Consequently, the development of intelligent anti-jamming methods capable of allowing UAVs to adaptively select carrier frequencies that suppress malicious jamming-induced channel interference is essential.

In light of the prevailing context, there is a pressing need to craft sophisticated anti-jamming strategies. These strategies should empower UAVs to dynamically choose center frequencies, effectively countering jamming from adversaries. At the heart of this initiative lies adaptive frequency modulation. In scholarly circles, a comprehensive, integrated approach is often advocated. This merges various methods and techniques, summarized as follows: (1) Spectrum Sensing and Dynamic Spectrum Access: UAVs utilize spectrum sensing to identify interference or vacant frequency bands [1–3]. Through Dynamic Spectrum Access (DSA), UAVs adapt in real-time to less crowded channels, reducing interference [4,5]; (2) Game Theory Approaches: Game theory models UAV interactions with wireless entities. Strategies are devised for UAVs to select frequencies adaptively, considering other users' behaviors to target optimal interference suppression [6–8]; (3) Machine Learning and AI: Algorithms predict and counteract interference. UAVs discern interference patterns, adjusting frequencies based on real-time insights and environmental factors, enhancing interference mitigation [9–11].

However, due to the inherent limitations of these methodologies, they cannot be directly applied to UAV-assisted A2G networks. In light of this, we introduce an innovative model for selecting central frequencies in UAV-jammer interactions within A2G networks. Unlike traditional studies, ours utilizes the Stackelberg game framework to enable UAVs to adaptively respond to dynamic jamming. By transforming this game into a concise linear programming approach, the study identifies optimal mixed-equilibrium strategies with polynomial time complexity, offering a novel solution for countering jamming attacks in UAV communication networks.

1.1. Related Work

In the above method, the inherent adversarial dynamics between a legitimate UAV and a malicious jammer have led to the widespread adoption of game-theoretical methodologies to model their competitive interactions. Existing game-theoretical approaches can be broadly categorized into two types: non-cooperative and hierarchical models.

Non-cooperative game models provide a mathematical lens to understand the simultaneous interactions between UAVs and jammers, anchored on the principle of Nash equilibrium solutions [12–20]. For instance, ref. [12] introduces a bimatrix game that sets out the conditions for a Nash equilibrium strategy within linear constraints. The study in [14] delves into channel coding in the face of adversarial jammers, revealing a convergence of game-theoretical and information-theoretical approaches in UAV communications over time. Meanwhile, the security challenges in cognitive radio networks, especially jamming attacks, are explored in [16], proposing game-theory-modeled anti-jamming strategies that utilize channel hopping and randomized power allocation. A passive anti-Primary User Emulation (PUE) approach, reminiscent of random frequency hopping, is discussed in [18]. Further, to address bandwidth and hardware limitations of FHSS signals, a channelized modulated wideband converter (MWC) scheme is proposed in [19]. Lastly, ref. [20] focuses on the distributed channel selection cooperative anti-jamming problem in UAV communication networks, suggesting an interference sensing cooperative anti-jamming scheme based on the Markov game framework. However, the non-cooperative game model presents challenges, including coordination issues, limitations in cluster networking adaptability, and difficulties in achieving convergence in expansive network settings.

In the intricate dance of spectrum jamming, the decision-making interplay between a transmitter and a jammer often adheres to a hierarchical sequence. This can be aptly represented through a Stackelberg game model. In this setup, the transmitter, assuming the role of the leader, orchestrates an optimal strategy, fully cognizant of the jammer's impending best response. A plethora of studies have ventured into crafting Stackelberg game solutions tailored for jamming attacks in wireless communications [21–30]. For instance, ref. [22] delves into power control dynamics, positioning the transmitter as the leader, empowered to select the optimal transmission power amidst a myriad of interference sources. Ref. [26] introduces an incentive mechanism, leveraging a coalitional game to galvanize legal UAVs into a coalition, with the Stackelberg game simulating the interplay between legal UAVs and adversaries. The findings underscore a marked enhancement in the anti-jamming prowess of UAV networks. Ref. [28] presents a game between a singular jammer and multiple users, pinpointing the Stackelberg equilibrium power dynamics. Moreover, ref. [29] harnesses a simulated annealing algorithm to discern the Stackelberg equilibrium, addressing power control intricacies within UAV communication networks' anti-interference framework. However, the Stackelberg game model grapples with challenges, such as reconciling the centralized leadership assumption with UAV networks' distributed essence and navigating uncertainties intrinsic to the Stackelberg paradigm.

The integration of artificial intelligence (AI) algorithms to counteract jamming communication dilemmas has garnered substantial traction. Jammers, endowed with learning capabilities, can fluidly recalibrate their jamming tactics, adeptly sensing the spectral milieu. This agility renders traditional anti-jamming mechanisms somewhat obsolete, catalyzing a shift towards AI-centric solutions [31–35]. For instance, ref. [32] reimagines power allocation challenges in adversarial contexts, crafting algorithms that approximate the Nash equilibrium between communicators and a jammer. Ref. [34] champions a hierarchical deep reinforcement learning algorithm, adeptly navigating frequency selection in jamming landscapes replete with frequency options. This algorithm adeptly sidesteps multifaceted jamming, ensuring commendable throughput. Such algorithms have showcased their mettle in curtailing the anticipated regret of communicators during real-time confrontations, all while maintaining operational prowess. Nevertheless, the computational intricacies of discerning the optimal frequency from an expansive spectrum remain a formidable challenge.

1.2. Motivations and Contributions

To comprehensively address the existing lacunae in the literature, the present paper elucidates a pioneering model tailored for the meticulous selection of central frequencies during adversarial interactions between UAVs and jammers within the realm of A2G networks. In a marked departure from conventional studies, our approach harnesses the power of the Stackelberg game framework, thereby enabling the UAV to exhibit an adaptive spectral response when confronted with dynamic jamming onslaughts. Through a meticulous transformation of this game into a sophisticated linear programming paradigm, we are able to ascertain optimal mixed equilibrium strategies that boast of polynomial time complexity. The methodology we advocate for not only showcases an elevated performance when juxtaposed with traditional paradigms like FHSS and RS but also excels in terms of communication payoff and robust stability. This superiority is further underscored through rigorous analytical evaluations and simulation-driven validations. The salient innovations of our study are delineated as follows:

(1) This study is at the forefront of revolutionizing central frequency selection optimization within Air-to-Ground (A2G) networks during adversarial UAV-jammer interactions. Departing significantly from conventional approaches, we harness the power of a Stackelberg game framework to empower UAVs with the ability to dynamically adapt their spectral responses. This innovative approach is strategically designed to effectively thwart dynamic jamming attacks and enhance the robustness of A2G communication networks;

(2) Our approach strategically utilizes the dual-matrix game method to effectively convert the intricate Stackelberg game into a more tractable linear programming problem. This strategic transformation plays a pivotal role in mitigating the computational complexities that are inherently embedded within the original game formulation. Through this methodological adjustment, we streamline the analytical process, rendering it more accessible and facilitating expedient decision-making, thus significantly contributing to the overarching objective of our study;

(3) In pursuit of our primary objective, we introduce an advanced algorithmic solution tailored to this linear programming problem. This approach has been rigorously validated and proven to deliver optimal mixed strategies efficiently within polynomial time. This remarkable achievement represents a substantial step forward, as it equips UAVs with the most advantageous mixed strategies, aligning with the core mission of our research—to enhance their operational effectiveness.

The subsequent structure of this paper is meticulously delineated as follows. In Section 2, we delve into a detailed exposition of both the system and communication models pertinent to UAVs. Section 3 is dedicated to the elucidation of the Bimatrix Stackelberg Game model, coupled with a discussion on the optimization objectives and the formulation of the optimal mixed strategy. Section 4 furnishes the reader with empirical numerical results, shedding light on the practical implications of our proposed methodologies. Finally, Section 5 offers a holistic recapitulation of the entire discourse, encapsulating the key takeaways and insights.

2. System Model and Problem Formulation

2.1. System Model

Figure 1 illustrates two scenarios involving the UAV, the receiver, and jammer. In the first scenario, the receiver is a stationary RSU, while, in the second scenario, the receiver is a moving vehicle. Our paper focuses on the analysis and discussion of these two distinct scenarios. The positions of the receivers and the jammer are measured using Cartesian coordinates, which can be denoted by $C_R^{'} = [c_{x_R}^{'}, c_{y_R}^{'}]$ and $C_J^{'} = [c_{x_J}^{'}, c_{y_J}^{'}]$, respectively. In terms of the moving UAV, let $C_U = [c_{x_U}, c_{y_U}, c_{z_U}]$ denote its position. While the jammer persistently emits jamming signals towards the UAV, the UAV simultaneously transmits messages to the receiver. At the beginning of each time slot, the UAV selects the communication center frequency f_U^c, and initiates the transmission of a signal to the receiver. Subsequently, the jammer, upon sensing the UAV's selected frequency f_U^c, chooses the center frequency f_J^c for its jamming signal.

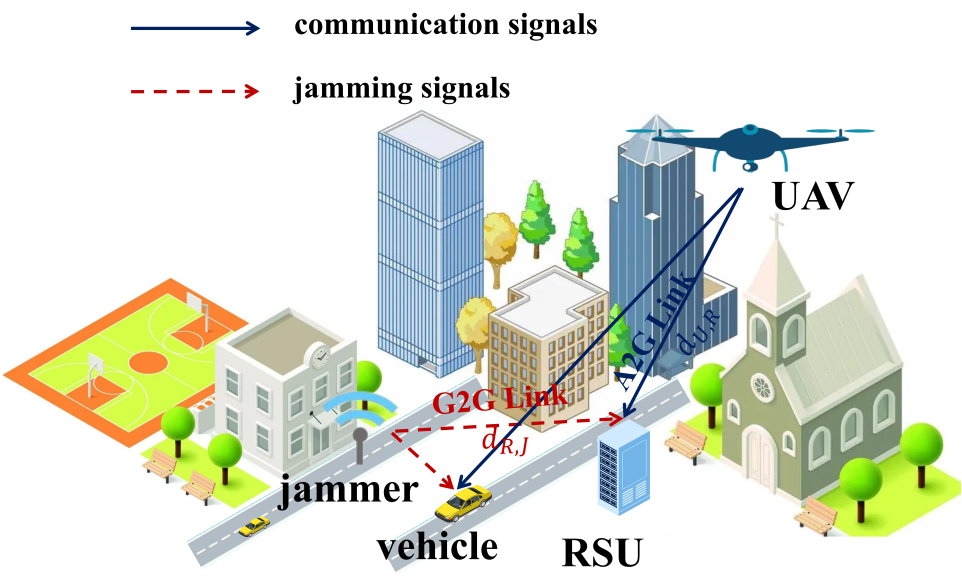

Figure 1. An A2G network in the presence of a jammer.

The transmission power of the UAV, denoted as P_U, remains constant throughout the communication process. In contrast, the channel gain between the UAV and the receiver, represented as g_U, is a function of various factors, including the distance between the communicating entities and the overall quality of the communication channel.

To accurately model the jamming interference within the communication environment, let $J(f)$ serve as the Power Spectrum Density (PSD) function explicitly associated with the jammer's transmitted signals. Likewise, g_J symbolizes the channel gain between the jammer and the UAV, which is an important metric in the overall system performance. Additionally, environmental noise plays a pivotal role and is also incorporated into the system model. This particular form of noise is quantitatively represented by the PSD function $N(f)$, and its inclusion in the model serves to offer a more comprehensive and realistic understanding of the intricate dynamics of real-world communication scenarios.

2.2. Communication Model

To shed light on the nuanced details of the frequency-selection problem at hand, we methodically partition the entire available frequency band B into M equally-sized sub-bands, each possessing a bandwidth delineated as $b = \frac{B}{M}$. Consequently, the range of communication bandwidth between the UAV and the receiver is strictly demarcated within the frequency range $[f_U^c - \frac{b}{2}, f_U^c + \frac{b}{2}]$. The UAV's center frequency f_U^c is ascertained by utilizing the mathematical formula $f_U^c = f_U^s + \frac{2n-1}{2}b$, where f_U^s designates the initial sensing frequency of the UAV, and n specifies the index of the n-th sub-band. Within the specialized context of wireless communication networks, the communication link that exists between the UAV and the receiver is conventionally termed an A2G link. Conversely, the link that connects the jammer to the receiver is categorized as a ground-to-ground (G2G) link. The spatial distance between the UAV and the receiver is denoted by

$$d_{U,R} = \sqrt{c_{z_U}^2 + \|[c_{x_U}, c_{y_U}] - [c'_{x_R}, c'_{y_R}]\|^2}, \tag{1}$$

and the distance between the receiver and the jammer is

$$d_{R,J} = \sqrt{\|[c_{x_R}, c_{y_R}] - [c'_{x_J}, c'_{y_J}]\|^2}, \tag{2}$$

where $\|\cdot\|$ represents the Euclidean norm. In the case of Line-of-Sight (LOS) communication, the channel gain g_U between the UAV and the receiver can be expressed as

$$g_U = g_{U0} d_{U,R}^{-\beta}, \tag{3}$$

and the channel gain g_J between the jammer and the receiver can be computed as

$$g_J = g_{J0} d_{U,J}^{-\beta}, \tag{4}$$

where g_{U_0} and g_{J_0} denote the reference channel gain at $d_{U,R} = d_{U,J} = 1$m, respectively, and $\beta \geq 2$ is the path loss exponent, with the assumption that the channel gain does not change during each time slot. The following is the received signal-to-jamming-plus-noise ratio (SJNR) from the UAV to the receiver:

$$\rho(f_U^c) = \frac{g_U P_U}{\int_{f_U^c - b/2}^{f_U^c + b/2} [N(f) + g_J J(f - f_J^c)] \mathrm{d}f}. \tag{5}$$

At the start of each time slot, the UAV determines the distance and quality of the communication channel between itself and the receiver. Simultaneously, the jammer performs the same action between itself and the UAV.

3. Bimatrix Stackelberg Game

3.1. Game Model

In the scenario described, the UAV initially selects its transmission center frequency, taking into account the jammer's potential actions. Subsequently, the jammer responds based on the UAV's chosen center frequency. This interaction aligns well with the Stackelberg game framework, prompting us to model the UAV and jammer's interactions using this game-theoretical approach. Specifically, since the UAV makes the initial decision, it acts as the leader in the game, while the jammer, responding to the UAV's actions, plays the role of the follower. Given that our scenario involves a single UAV and one jammer, they collectively represent the participants in the game. The game is formally defined as

$$\mathcal{G} = \{\mathcal{U}, \mathcal{J}, \mathcal{F}_U^c, \mathcal{F}_J^c, \mathcal{U}_U, \mathcal{U}_J\}, \tag{6}$$

where $\mathcal{F}_U^c$ and $\mathcal{F}_J^c$ represent the action sets of the UAV and the jammer, respectively. The UAV's frequency selection is denoted by $f_U^c \in \{f_{U1}^c, f_{U2}^c, \ldots, f_{UM}^c\}$, while the jammer's frequency selection action is represented by $f_J^c \in \{f_{J1}^c, f_{J2}^c, \ldots, f_{JM}^c\}$. The utility functions $\mathcal{U}_U$ and $\mathcal{U}_J$ for the UAV and the jammer, respectively, are derived from the signal-to-jamming-plus-noise Ratio (SJNR) received by the receiver. These utility functions can be expressed as follows:

$$u_U(f_U^c, f_J^c) = \frac{g_U P_U}{\int_{f_U^c - b/2}^{f_U^c + b/2} [N(f) + g_J J(f - f_J^c)] \mathrm{d}f} - \lambda_1 P_U, \tag{7}$$

$$u_J(f_U^c, f_J^c) = -\frac{g_U P_U}{\int_{f_U^c - b/2}^{f_U^c + b/2} [N(f) + g_J J(f - f_J^c)] \mathrm{d}f} - \lambda_2 P_J, \tag{8}$$

where transmission power of the UAV is denoted by P_U and the jammer's transmission power is represented by $P_J = \int_{f_J^s}^{f_J^s + (M-1)b} J(f) \mathrm{d}f$. The variables λ_1 and λ_2 signify the transmission costs per unit power for the UAV and the jammer, respectively.

3.2. Optimization Objectives

The UAV is driven by the objective to optimize its communication quality, an endeavor which is mathematically expressed by the goal of maximizing its utility function:

$$\begin{aligned} &\max u_U(f_U^c), \\ &\text{s.t.} \quad f_U^c \in \mathcal{F}_U^c. \end{aligned} \tag{9}$$

Conversely, the jammer's objective is to minimize the communication quality between the UAV and the receiver, effectively maximizing its own utility function:

$$\begin{aligned} &\max u_J(f_U^c), \\ &\text{s.t.} \quad f_J^c \in \mathcal{F}_J^c. \end{aligned} \tag{10}$$

In accordance with the Stackelberg game's characteristics, the optimization problems for both the UAV and the jammer must be coupled to derive the final optimization problem:

$$\begin{aligned} &\max u_U(f_U^c, f_J^{c*}), \\ &\text{s.t.} \begin{cases} f_J^{c*} = \arg\max u_J(f_J^c), \\ f_U^c \in \mathcal{F}_F^c, \\ f_J^c \in \mathcal{F}_J^c. \end{cases} \end{aligned} \tag{11}$$

3.3. Optimal Mixed Strategy for UAV

The Stackelberg game articulated in Problem (11) can be reformulated as a binary integer programming problem. Such problems are generally NP-hard, posing computational challenges. According to the minimax theorem [36], a set of mixed strategies in zero-sum games is a Nash equilibrium if and only if both strategies are minimax strategies. It is well-established that linear programming can efficiently find such minimax strategies within polynomial time [37].

After spectrum sensing, the UAV and the jammer construct their respective payoff matrices, denoted as $\boldsymbol{A}$ and $\boldsymbol{B}$. These matrices are defined as

$$\boldsymbol{A} = \begin{bmatrix} u_U(f_{U1}^c, f_{J1}^c) & \cdots & u_U(f_{U1}^c, f_{JM}^c) \\ \vdots & \ddots & \vdots \\ u_U(f_{UM}^c, f_{J1}^c) & \cdots & u_U(f_{UM}^c, f_{JM}^c) \end{bmatrix}, \tag{12}$$

$$B = \begin{bmatrix} u_J(f^c_{U1}, f^c_{J\,1}) & \cdots & u_J(f^c_{U1}, f^c_{J\,M}) \\ \vdots & \ddots & \vdots \\ u_J(f^c_{U\,M}, f^c_{J\,1}) & \cdots & u_J(f^c_{U\,M}, f^c_{J\,M}) \end{bmatrix}. \tag{13}$$

Leveraging the principles of the minimax theorem, the complex interaction that transpires between the UAV and the jammer at the onset of each discrete time slot is elegantly reformulated into a bimatrix Stackelberg game framework. Within this mathematical setting, the pursuit of identifying an optimal mixed strategy for the UAV effectively becomes synonymous with discovering a minimax strategy, a strategy that seeks to minimize the maximum expected utility, symbolically represented as u_J, which the adversarial jammer can potentially attain.

Theorem 1. *In the game of the UAV and the jammer, an optimal mixed strategy to which to commit can be found in polynomial time using linear programming.*

Proof of Theorem. For the jammer's every pure strategy, i.e.,

$$\pi_J \in \Pi_J = \underbrace{[1,0,\cdots,0]^T, [0,1,0,\cdots,0]^T, \cdots, [0,\cdots,0,1]^T}_{M}, \tag{14}$$

where M is the total number of strategies and 1 indicates that the jammer may choose the corresponding center frequency f^c_J, we compute a mixed strategy for the UAV:

$$\pi_U = [p_{f^c_{U1}}, p_{f^c_{U2}}, \cdots, p_{f^c_{U\,m}}, \cdots, p_{f^c_{U\,M}}]^{\mathrm{T}}, \tag{15}$$

where $p_{f^c_{U\,m}}$ represents the probability that the UAV would choose the center frequency $f^c_{U\,m}$, with $\sum_{m=1}^{M} p_{f^c_{U\,m}} = 1$. Two prerequisites must be satisfied: (1) playing π_J is the best response for the jammer, and (2) the mixed strategy maximizes the UAV's utility under constraint (1). Such a mixed strategy can be produced by the following linear program:

$$\begin{aligned} &\max_{\pi_U \in \Pi_U} \quad \sum_{m=1}^{M} p_{f^c_{U\,m}} u_U(f^c_{U\,m}, f^c_{J\,\pi_J}), \\ &\text{s.t.} \begin{cases} \sum_{m=1}^{M} p_{f^c_{U\,m}} u_J(f^c_{U\,m}, f^c_J) \geq \sum_{m=1}^{M} p_{f^c_{U\,m}} u_J(f^c_{U\,m}, f^{c'}_J), \\ \sum_{m=1}^{M} p_{f^c_{U\,m}} = 1, \\ p_{f^c_{U_m}} \geq 0. \end{cases} \end{aligned} \tag{16}$$

For each possible strategy $\pi_J \in \Pi_J$ of the jammer, the UAV considers it as the jammer's optimal response, meaning that the jammer's payoff from selecting the central frequency f^c_J is greater than payoffs of any other central frequency $f^{c'}_J$. Then, the UAV computes the corresponding optimal mixed strategy. Among all the optimal objective function values obtained, the UAV selects the one that maximizes its own payoff as the final optimal payoff. The corresponding mixed strategy represents the optimal strategy for the UAV, while the pure strategy represents the optimal response strategy for the jammer. □

3.4. *Algorithm Design and Analysis*

As delineated in Algorithm 1, the proposed computational framework commences each time slot by quantitatively assessing the Euclidean distances between the UAV, the designated receiver RSU, and the adversarial jammer.

Algorithm 1 Algorithm for solving mixed strategies.

Input: $t = 0$, the position of the UAV C_U, the receiver $C_R^{'}$, and the jammer $C_J^{'}$
Output: optimal mixed strategy for UAV π_U^* at every time slot

for $t = 0, \ldots, T$ **do**
  Compute g_U and g_J based on $d_{U,R}$ and $d_{U,J}$
  Calculate the payoff matrix $\boldsymbol{A}$ and $\boldsymbol{B}$
  for $\pi_J = 1, \ldots, M$ **do**
    $\pi_U^{can} \leftarrow \arg \min_{\pi_U \in \Pi_U} [-\sum_{m=1}^{M} p_{f_{Um}^c} u_U(f_{Um}^c, f_{J\,\pi_J}^c)]$
    $P_{\pi_U^{can}} \leftarrow \sum_{m=1}^{M} p_{f_{Um}^c}^{\pi_U^{can}} u_U(f_{Um}^c, f_{J\,\pi_J}^c)$
  end for
  Select π_U^* from Π_U^{can} with $P_{\pi_U^{can}}^*$
end for

These computed spatial metrics serve as the foundational parameters upon which the algorithm constructs the respective payoff matrices, denoted as $\boldsymbol{A}$ and $\boldsymbol{B}$. Specifically, $\boldsymbol{A}$ is constructed as a matrix with column vectors $[\boldsymbol{\alpha}_1, \ldots, \boldsymbol{\alpha}_M]$, while $\boldsymbol{B}$ is formulated as $[\boldsymbol{\beta}_1, \ldots, \boldsymbol{\beta}_M]$. For example, in vector $\boldsymbol{\alpha}_m$, each element quantifies the utility the UAV gains upon selecting various center frequencies, given that the jammer adopts the m-th center frequency. Subsequently, for each identified pure strategy π_J available to the jammer, the algorithm rigorously determines the UAV's corresponding optimal mixed strategy by solving a well-posed linear programming problem.

To effectively tackle the linear programming complexities outlined in Algorithm 1, we introduce Algorithm 2. The developed method serves as a robust and computationally proficient framework specifically tailored to address the linear programming challenges presented in Algorithm 1. After performing a series of mathematical manipulations, including the inversion of the original objective function and the introduction of slack variables, Problem (16) is meticulously transformed into its standard form, indicated as

$$\min {\boldsymbol{\alpha}_m^s}^{\mathrm{T}} \boldsymbol{x},$$
$$\text{s.t.} \begin{cases} \boldsymbol{C}\boldsymbol{x} = 0, \\ \sum_{m=1}^{2M-1} \boldsymbol{x}_m = 1, \\ \boldsymbol{x} = \begin{bmatrix} \pi_U \\ \boldsymbol{s} \end{bmatrix}, \boldsymbol{x} \in \mathbb{R}^{2M-1}, \\ \boldsymbol{x} \geq 0, \\ \boldsymbol{\alpha}_m^s = \begin{bmatrix} \boldsymbol{\alpha}_m \\ 0 \\ \vdots \\ 0 \end{bmatrix}, \boldsymbol{\alpha}_m^s \in \mathbb{R}^{2M-1}, \end{cases} \tag{17}$$

where $\boldsymbol{s}$ as a set of slack variables, given the inequality constraints inherent in the original problem (16). These variables are seamlessly integrated into the decision variable π_U from the original problem, leading to the composite formation of $\boldsymbol{x}$. Within this context, $\boldsymbol{\alpha}_m^s$ denotes the coefficient in the objective function following the inclusion of the slack variable, ensuring that all coefficients corresponding to these slack variables remain consistently zero. The coefficient matrix $\boldsymbol{C}$ is displayed as follows:

$$\boldsymbol{C} = \begin{bmatrix} \boldsymbol{\beta}_m - \boldsymbol{\beta}_1 & -1 & \cdots & 0 & 0 & 0 & \cdots & 0 \\ \vdots & & & & & & & \\ \boldsymbol{\beta}_m - \boldsymbol{\beta}_{m-1} & 0 & \cdots & -1 & 0 & 0 & \cdots & 0 \\ \boldsymbol{\beta}_m - \boldsymbol{\beta}_{m+1} & 0 & \cdots & 0 & 0 & -1 & \cdots & 0 \\ \vdots & & & & & & & \\ \boldsymbol{\beta}_m - \boldsymbol{\beta}_M & 0 & \cdots & 0 & 0 & 0 & \cdots & -1 \end{bmatrix}, \boldsymbol{C} \in \mathbb{R}^{(M-1)\times(2M-1)}, \tag{18}$$

where the matrix $\boldsymbol{C}$ is the standardized coefficient matrix. This matrix elucidates that, when the jammer adopts any strategy other than the m-strategy, the resultant payoff will invariably not exceed that achieved by adopting the m-strategy. This solidifies the hypothesis that selecting the m-strategy emerges as the jammer's optimal response.

Through projective transformation, the optimization problem in (17) is converted into a sphere domain where minimization occurs. After finding the optimal solution in the sphere domain, an inverse transformation maps this solution back to the original decision space, thus approximating the solution of the initial problem. This iterative process eventually results in an optimal $p_{f_U^c}$ that converges in polynomial time. Subsequently, the transformation process of Problem (17) is analyzed in detail.

The feasible region is the intersection of subspace $\{\Phi = \boldsymbol{x}|\boldsymbol{\alpha}_m^{s\,\mathrm{T}}\boldsymbol{x} = 0\}$ and simplex $\boldsymbol{S} = \{\boldsymbol{x}|\sum_{j=1}^{2M-1}\boldsymbol{x}_j = 1, \boldsymbol{x} \geq 0\}$, so Problem (17) can be expressed as

$$\begin{aligned} &\min \boldsymbol{\alpha}_m^{s\,\mathrm{T}}\boldsymbol{x}, \\ &\text{s.t. } \boldsymbol{x} \in \boldsymbol{S} \cap \Phi. \end{aligned} \tag{19}$$

Moreover, the subspace Φ is transformed into Φ' by transformation $T(\boldsymbol{x}) = \frac{\boldsymbol{D}^{-1}\boldsymbol{x}}{\boldsymbol{e}^{\mathrm{T}}\boldsymbol{D}^{-1}\boldsymbol{x}}$, and $\boldsymbol{S}$ is transformed into $\boldsymbol{S}'$. Thus, the feasible region converts from $\boldsymbol{S} \cap \Phi$ into $\boldsymbol{S}' \cap \Phi'$. Simultaneously, this transformation alters the point $\boldsymbol{a} = (a_1, \cdots, a2M-1)^{\mathrm{T}} > 0$ on the simplex $\boldsymbol{S}$ into the midpoint $\boldsymbol{a}^0 = \frac{1}{n}\boldsymbol{e}$ of the simplex $\boldsymbol{S}'$. Clearly, $\boldsymbol{a}^0$ belongs to $\boldsymbol{S}' \cap \Phi'$. After transformation, the objective function $\boldsymbol{\alpha}^s m^{\mathrm{T}}\boldsymbol{x}$ becomes a fractional function $\frac{\boldsymbol{\alpha}^s m^{\mathrm{T}} D x'}{\boldsymbol{e}^{\mathrm{T}} D x'}$. Consequently, Equation (20) serves as a substitute for the original objective function $\boldsymbol{\alpha}^s m^{\mathrm{T}}\boldsymbol{x}$, and $h(\boldsymbol{x})$ is transformed into $h'(\boldsymbol{x})$, which are displayed below, respectively:

$$h(\boldsymbol{x}) = \sum_{j=1}^{2M-1} \ln \frac{l(\boldsymbol{x})}{\boldsymbol{x}_j}, l(\boldsymbol{x}) = \boldsymbol{\alpha}_m^{s\,\mathrm{T}}\boldsymbol{x}^k, \tag{20}$$

$$h'(\boldsymbol{x}) = \sum_{j=1}^{2M-1} \ln \frac{\boldsymbol{\alpha}_m^{s\,\prime\mathrm{T}}\boldsymbol{x}'}{\boldsymbol{x}'_j} - \sum_{j=1}^{2M-1} \ln a_j. \tag{21}$$

The main purpose of employing $h(x)$ is to facilitate the minimization of the original objective function through the minimization of this potential function, thereby enabling efficient optimization techniques. In this manner, Problem (19) is transformed into Problem (22):

$$\begin{aligned} &\min h'(\boldsymbol{x}'), \\ &\text{s.t. } \boldsymbol{x}' \in \boldsymbol{S}' \cap \Phi'. \end{aligned} \tag{22}$$

For ease of calculation, a sphere $\boldsymbol{S}'$ with $\boldsymbol{a}^0$ as the center and ηr as the radius contained in the simplex $\boldsymbol{S}'$ is used instead of $\boldsymbol{S}$, where r is the radius of the inscribed circle of the simplex $\boldsymbol{S}$ and $r = \frac{1}{\sqrt{(2M-1)(2M-2)}}, \zeta \in (0,1)$. It is important to note that the constant δ is related to the value of ζ, and the relationship between these two parameters is

$$\delta = \zeta - \frac{\zeta^2}{2} - \frac{\zeta^2 n}{(2M-2)[1-\zeta\sqrt{(2M-1)(2M-2)}]}. \tag{23}$$

Since the center $\boldsymbol{a}^0$ of the sphere $\boldsymbol{F}(\boldsymbol{a}^0, \zeta r)$ is already located within the transformed subspace $\Phi^{'}$, the resultant intersection between this sphere and the subspace forms a reduced-dimensional sphere. This new sphere retains $\boldsymbol{a}^0$ as its center and maintains the original radius ζr. Mathematically, this intersected, reduced-dimensional sphere can be denoted as

$$\boldsymbol{F}^{'}(\boldsymbol{a}^0, \zeta r) = \boldsymbol{F}(\boldsymbol{a}^0, \zeta r) \cap \Phi^{'}, \tag{24}$$

and each element $\boldsymbol{x}^{'}$ in $\boldsymbol{F}^{'}(\boldsymbol{a}^0, \zeta r)$ satisfies

$$\boldsymbol{A}\boldsymbol{D}\boldsymbol{x}^{'} = 0, \tag{25}$$

$$\sum_{j=1}^{2M-1} \boldsymbol{x}^{'} = 1, \text{i.e.}, \boldsymbol{e}^{\mathrm{T}}\boldsymbol{x}^{'} = 1. \tag{26}$$

Now, expand the matrix $\boldsymbol{CD}$, so that

$$\boldsymbol{F} = \begin{bmatrix} \boldsymbol{CD} \\ e^T \end{bmatrix}, \tag{27}$$

where $e^T = (1, \cdots, 1)$ is an n-dimensional vector with all components equal to 1, which can be expressed as

$$\boldsymbol{e}_{n+1} = \begin{bmatrix} 0 \\ 1 \end{bmatrix}, \tag{28}$$

where $\boldsymbol{e}_{n+1}$ is an $n+1$ -dimensional vector whose first n components are 0. In this way, Equations (25) and (26) can be expressed as $\boldsymbol{F}\boldsymbol{x}^{'} = \boldsymbol{e}_{n+1}$. Obviously, $\boldsymbol{F}^{'}(\boldsymbol{a}^0, \zeta r)$ is a sphere in affine space $\Phi^{''} = \{\boldsymbol{x}^{'} | \boldsymbol{F}\boldsymbol{x}^{'} = \boldsymbol{e}_{n+1}\}$. Thus, Problem (22) turns into

$$\begin{aligned} &\min h^{'}(\boldsymbol{x}^{'}), \\ &\text{s.t. } \boldsymbol{x}^{'} \in F^{'}(\boldsymbol{a}^0, \zeta r) \cap \Phi^{''}. \end{aligned} \tag{29}$$

Ultimately, the potential minimization function h' can be closely approximated by the linear function $\boldsymbol{\alpha}_m^{s\ 'T}\boldsymbol{x'}$. Consequently, Equation (29) can be reformulated as the optimization problem delineated in Equation (30):

$$\begin{aligned} &\min \boldsymbol{\alpha}_m^{s\ 'T}\boldsymbol{x'}, \\ &\text{s.t.}\boldsymbol{x'} \in F'(\boldsymbol{a^0}, \zeta r) \cap \Phi'', \end{aligned} \tag{30}$$

where $\boldsymbol{\alpha}_m^{s\ '} = \boldsymbol{D}\boldsymbol{\alpha}_m^s$.

To ascertain the minimizer of the function $\boldsymbol{\alpha}_m^{s\ 'T}\boldsymbol{x'}$ over the set $\boldsymbol{F}$, consider that this set constitutes a sphere in the affine space Φ'', centered at $\boldsymbol{a^0}$. Given that $\boldsymbol{\alpha}_m^{s\ 'T}\boldsymbol{x'}$ is a linear function, one can initiate the search from $\boldsymbol{a^0}$ and move along the direction where $\boldsymbol{\alpha}_m^{s\ 'T}\boldsymbol{x'}$ decreases most rapidly in Φ''. The optimal step length for this move is ζr. Consequently, the point at which the function reaches its minimum is determined.

The steepest descent direction in Φ'' corresponds to the projection of the most negative gradient $-\boldsymbol{\alpha}_m^{s\ 'T}$ in the null space $N(\boldsymbol{F})$ of $\boldsymbol{F}$, defined as $N(\boldsymbol{F}) = \{\boldsymbol{x'} | \boldsymbol{F}\boldsymbol{x'} = 0\}$. Assuming that $\boldsymbol{F}$ is of full rank, this projection, $\boldsymbol{\alpha}_{mp}^s$, can be calculated as

$$\boldsymbol{\alpha}_{mp}^s = [\boldsymbol{I} - \boldsymbol{B}^T(\boldsymbol{B}\boldsymbol{B}^T)^{-1}\boldsymbol{B}]\boldsymbol{D}\boldsymbol{\alpha}_m^s. \tag{31}$$

Subsequently, the fastest descending direction d^0 is given by $d^0 = -\frac{\boldsymbol{\alpha}_{mp}^s}{\|\boldsymbol{\alpha}_{mp}^s\|}$. The minimal point b' on the reduced-dimensional sphere $\boldsymbol{F'}$ corresponds to $a^0 - \frac{\zeta r}{\|\boldsymbol{\alpha}_{mp}^s\|}\boldsymbol{\alpha}_{mp}^s$.

To obtain an approximate solution to Equation (19), one can find the pre-image of $\boldsymbol{F'}$ through inverse transformation to yield b. This point b can then be mapped to the centroid of the simplex S', facilitating the resolution of Equation (22). Iterative application of this methodology results in an optimal solution that converges to that in Equation (19) and, ultimately, to Equation (17), thereby determining the optimal mixed strategy for the UAV. Details of this algorithmic procedure are elucidated in Algorithm 2.

Upon employing Algorithm 2 to discern the optimal decision corresponding to each possible center frequency utilized by the jammer, the UAV proceeds to a higher-level optimization. Among the array of optimal strategies thus identified, the UAV selects the one that yields the maximum individual payoff. This strategic choice enables the UAV to attain the highest expected communication revenue.

Theorem 2. *Algorithm 2 is designed to efficiently identify a feasible point* $\mathbf{x}$ *within a computational complexity of* $O\{(2M-1)[q+\ln(2M-1)]\}$ *steps, thereby ensuring that* $\frac{{\boldsymbol{\alpha}_m^s}^{\mathrm{T}}\boldsymbol{x}^k}{{\boldsymbol{\alpha}_m^s}^{\mathrm{T}}\boldsymbol{a}^0} \leq 2^{-q}$ *holds true. This computational efficiency enables the rapid convergence to an approximate yet highly effective solution for the underlying optimization problem.*

Algorithm 2 Algorithm for solving standardized linear programming problem.

Input: $k=0$, Given the parameter value $\zeta \in (0,1)$, Termination Criterion q, Initial solution $\boldsymbol{x}^0 = \boldsymbol{a}^0 = \frac{1}{2M-1}(1,\cdots,1)^{\mathrm{T}}$, Assumed optimal response $f_{J\,m}^c$

Output: Optimal mixing strategy $P_{\pi_U^{can}}$ of the UAV for $f_{J\,m}^c$

1: **for** $k = 0, \ldots$ **do**

2:     **if** $\frac{{\boldsymbol{\alpha}_m^s}^{\mathrm{T}}\boldsymbol{x}^k}{{\boldsymbol{\alpha}_m^s}^{\mathrm{T}}\boldsymbol{a}^0} > 2^{-q}$

3:         $\boldsymbol{D} \leftarrow \mathrm{diag}(x_1^k,\cdots,x_{2M-1}^k)$

4:         $\boldsymbol{F} \leftarrow \begin{bmatrix} \boldsymbol{CD} \\ e^T \end{bmatrix}, e^T = (1,\cdots,1)$

5:         Calculate the projection of gradient ${\boldsymbol{\alpha}_m^s}'$ in the null space of $\boldsymbol{F}$:
$\boldsymbol{\alpha}_{mp}^s \leftarrow [\boldsymbol{I} - \boldsymbol{B}^T(\boldsymbol{BB}^T)^{-1}\boldsymbol{B}]{\boldsymbol{\alpha}_m^s}'$

6:         Calculate the unitized $\boldsymbol{\alpha}_{mp}^s$: $\boldsymbol{\alpha}_m^{\hat{s}} \leftarrow \frac{\boldsymbol{\alpha}_{mp}^s}{\|\boldsymbol{\alpha}_{mp}^s\|}$

7:         Compute the minimum point on the sphere $\boldsymbol{b}' \leftarrow \boldsymbol{a}^0 - \frac{\zeta}{\sqrt{(2M-1)(2M-2)}}\boldsymbol{\alpha}_m^{\hat{s}}$

8:         **if** $h(\boldsymbol{x}^k) - h(\boldsymbol{x}^{k+1}) \geq \delta$

9:             $k \leftarrow k+1$

10: **end for**

Proof of Theorem. For each k, we have

$$\begin{aligned} h(\boldsymbol{x}^{k+1}) &\leq h(\boldsymbol{x}^k) - \delta, \\ h(\boldsymbol{x}^k) &\leq h(\boldsymbol{x}^0) - k\delta, \\ \sum_{j=1} \ln \frac{{\boldsymbol{\alpha}_m^s}^{\mathrm{T}}\boldsymbol{x}^k}{\boldsymbol{x}_j^k} &\leq \sum_{j=1} \ln \frac{{\boldsymbol{\alpha}_m^s}^{\mathrm{T}}\boldsymbol{a}_j^0}{\boldsymbol{a}_j^0} - k\delta, \\ (2M-1)\ln \frac{{\boldsymbol{\alpha}_m^s}^{\mathrm{T}}\boldsymbol{x}^k}{{\boldsymbol{\alpha}_m^s}^{\mathrm{T}}\boldsymbol{a}^0} &\leq \sum_{j=1} \ln(x_j^k) - \sum_{j=1} \ln a_j^0 - k\delta, \end{aligned} \tag{32}$$

where δ is consistent with the parameter delineated in (23); this implies that, when an optimal solution exists, the reduction in the potential function is no less than the constant δ. Given that $\boldsymbol{x}_j^k \leq 1$ and $\boldsymbol{a}_j^0 = \frac{1}{2M-1}$, we can deduce that $\ln \frac{{\boldsymbol{\alpha}_m^s}^{\mathrm{T}}\boldsymbol{x}^k}{{\boldsymbol{\alpha}_m^s}^{\mathrm{T}}\boldsymbol{a}^0} \leq \ln(2M-1) - \frac{k}{2M-1}\delta$.

Subsequently, we conclude that there exits a constant $k^{'}$ such that, after $k^{'}(2M-1)[q+\ln(2M-1)]$ interactions, the inequality $\frac{{\boldsymbol{\alpha}_m^s}^{\mathrm{T}}\boldsymbol{x}^k}{{\boldsymbol{\alpha}_m^s}^{\mathrm{T}}\boldsymbol{a}^0} \leq 2^{-q}$ holds true. $\square$

One notable advantage of this algorithm is its computational efficiency, capable of identifying the optimal mixed strategy for the UAV in polynomial time. This efficiency is particularly crucial for real-time applications and enhances the physical layer security in A2G communication networks.

4. Simulation Results and Discussions

4.1. Simulation Parameters

The algorithms proposed in this study have undergone rigorous testing through simulation experiments across a spectrum range spanning from 100 MHz to 200 MHz. The meticulous parameter settings employed throughout our simulations are comprehensively outlined in Table 1. Unless explicitly stated otherwise, these settings remain consistent across all the conducted simulation experiments. For the sake of detailed analysis, we partition the total available bandwidth $\boldsymbol{B}$ into $M = 25$ distinct sub-bands, each possessing a bandwidth of $b = 4$ MHz. Consequently, the action sets for both the UAV and the jammer are delineated as $\mathcal{F}_U^c, \mathcal{F}_J^c = \{102\,\mathrm{MHz}, 106\,\mathrm{MHz}, \ldots, 198\,\mathrm{MHz}\}$, with cardinalities $|\mathcal{F}_U^c| = |\mathcal{F}_J^c| = 25$.

Table 1. Simulation Parameters.

Parameters	Notation	Value
UAV sensing start frequency	f_U^s	100 MHz
Total bandwidth	B	100 MHz
Sub-bands' number	M	25
UAV's transmission power	P_U	15 dBm
UAV's transmission cost	λ_1	0.5
Jammer's transmission cost	λ_2	0.25
Roll-off factor	η	0.4
Channel gain at the one-meter distance	$g_{U0}; g_{J0}$	−60 dBm
Path loss exponent	β	3
Gaussian white noise PSD $N(f)$	δ^2	−110 dBm
Parameter in the standard linear programming	ζ	0.25

4.2. Performance Comparison

To better simulate real-world conditions, we have crafted two distinct simulation scenarios, visually depicted in Figure 2. In Scenario 1, the UAV follows a circular trajectory above both the RSU and the jammer, with the RSU functioning as the receiver. Conversely, in Scenario 2, the UAV trails the trajectory of a dynamically moving vehicle, wherein the vehicle serves as the designated receiver. These carefully constructed scenarios facilitate a thorough evaluation and subsequent analysis of the UAV and jammer's performance in varying operational contexts.

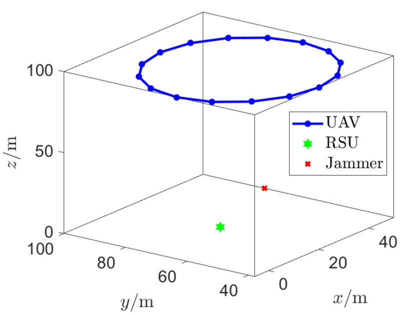

(a) Scenario 1

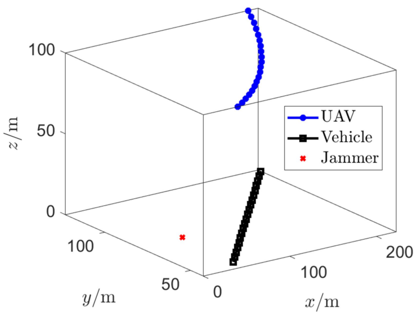

(b) Scenario 2

Figure 2. The UAV trajectory and the receiver's position in different scenarios.

Figure 3 demonstrates that in Scenario 1, neither the UAV nor the jammer can enhance their respective payoffs by independently adjusting their strategies. Correspondingly, Figure 4 elucidates that in Scenario 2, both the UAV and the jammer are incapable of augmenting their communication revenue through unilateral strategic modifications.

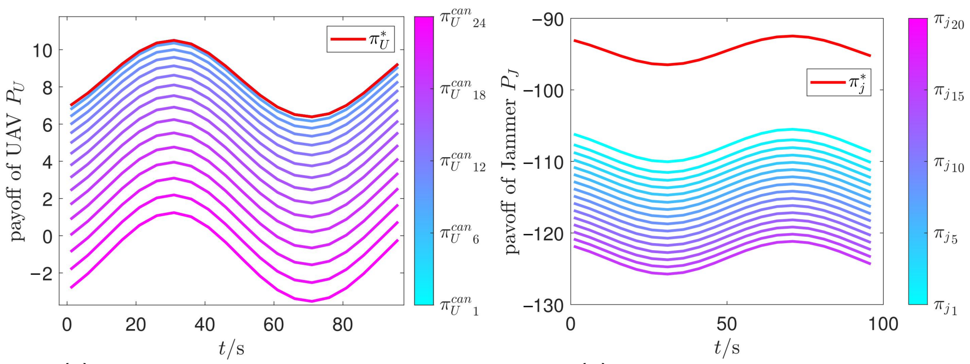

(a) The UAV's payoff variation from the UAV's strategy change. (b) The jammer's payoff variation from the jammer's strategy change.

Figure 3. Scenario 1 model validation.

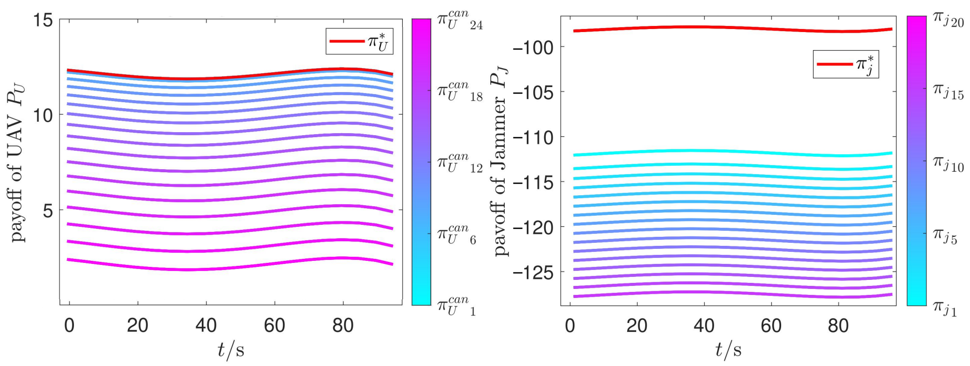

(a) The UAV's payoff variation from the UAV's strategy change. (b) The jammer's payoff variation from the jammer's strategy change.

Figure 4. Scenario 2 model validation.

These observations imply that, within this particular strategy set, any player who unilaterally changes its strategy—while keeping the other player's strategy constant—will not achieve an increase in its individual payoff. This provides compelling evidence that the derived strategies constitute a Nash equilibrium.

Figure 5 substantiates the superior payoff and stability of our proposed method in comparison to Frequency-Hopping Spread Spectrum (FHSS) and Random Selection (RS). In Scenario 1, our approach yields an average UAV communication payoff that exceeds FHSS by 13.5 and RS by 15.2. Similarly, in Scenario 2, our method surpasses FHSS by an average of 11.1 and RS by 9.4 in UAV communication payoff. These results underscore the efficacy of our approach in augmenting UAV communication performance, particularly in outclassing FHSS and RS under dynamic conditions.

As illustrated in Figure 6, it becomes apparent that increasing the number of sub-bands—thereby reducing the bandwidth of each—yields higher payoffs for the UAV. This enhancement can be attributed to the increased complexity the jammer faces in disrupting the corresponding signaling channels when more sub-bands are available. Consequently, the UAV gains a strategic advantage as the jammer struggles to execute effective attacks, leading to improved communication performance and elevated payoffs for the UAV. Furthermore, across various scenarios with different sub-bandwidths, our proposed algorithm consistently achieves the highest communication benefits. This advantage becomes increasingly pronounced as the sub-bandwidth expands. Specifically, when the sub-bandwidth is set to 5 MHz, the average payoff of our proposed method surpasses that of the FHSS method by 16.8 and the RS method by 17.1.

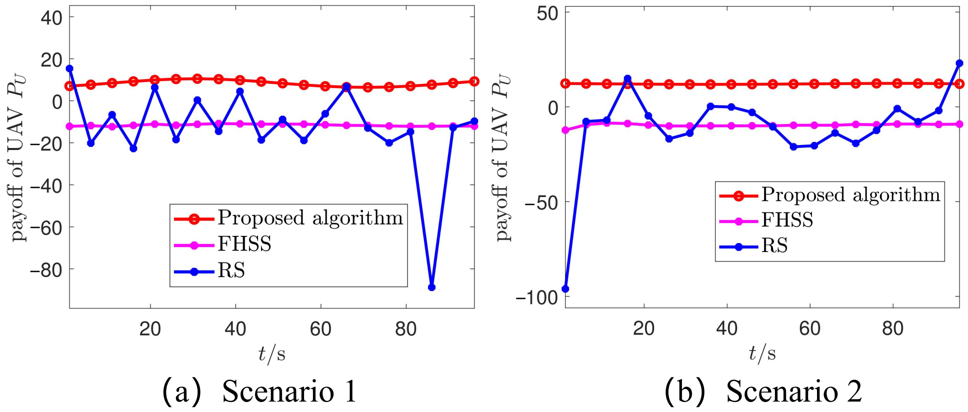

Figure 5. The communication payoffs of the UAV in different scenarios.

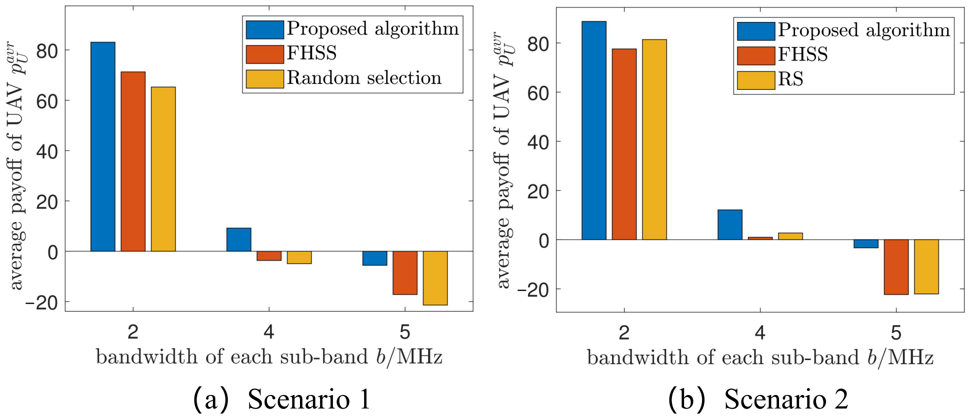

Figure 6. The impact of sub-bandwidth on communication payoff of the UAV.

5. Conclusions

This study tackles the challenge of center frequency selection for unmanned aerial vehicles (UAVs) faced with jamming attacks by employing a bimatrix Stackelberg game framework. We model the interaction between the UAV and the jammer as a Stackelberg game, subsequently transforming it into a bimatrix formulation to ascertain the UAV's optimal mixed strategy. Furthermore, we craft a linear programming solution algorithm. We provide a rigorous proof demonstrating that this algorithm is capable of determining the UAV's mixed strategy against each individual strategy employed by the jammer, all within polynomial time complexity. Ultimately, this facilitates the derivation of the UAV's optimal mixed strategy. The efficacy of our approach is corroborated through simulation experiments, which confirm convergence to a Nash equilibrium.

Our simulation results compellingly demonstrate that the proposed method significantly outperforms existing alternatives, such as Frequency-Hopping Spread Spectrum (FHSS) and Random Selection (RS), in terms of both stability and payoff in A2G communication scenarios. By adeptly selecting the optimal center frequency for the UAV, our approach effectively neutralizes the adverse impact of jamming attacks and optimizes communication efficiency. Utilizing the Stackelberg game framework and achieving convergence to the Nash equilibrium, this research offers valuable insights and practical implications for the judicious selection of UAV center frequencies in jamming-prone environments, thereby enhancing the overall performance and reliability of A2G communications.

In our study, we focused on a scenario with a singular receiver and jammer. While this provides insights, it might not encapsulate the intricacies of real-world environments where interactions among multiple transmitters and jammers are commonplace. Recognizing this constraint, our future endeavors aim to broaden the scope by incorporating multiple jammers and receivers. Such an extension will furnish a holistic assessment of our algorithm's resilience to jamming, especially in multifaceted interference landscapes with numerous transmitters.

Author Contributions: Conceptualization, L.C., D.T. and X.D.; methodology, L.C. and Z.X.; software, L.C., Z.X., and D.T.; validation, D.Z. and L.C.; formal analysis, L.C. and J.Z.; investigation, K.Q.; resources, X.D. and D.Z.; data curation, L.C. and X.D.; writing—original draft preparation, L.C. and Z.X.; writing—review and editing, D.Z.; visualization, L.C., D.T. and K.Q.; supervision, Z.X.; project administration, J.Z.; funding acquisition, D.T. and J.Z. All authors have read and agreed to the published version of the manuscript.

Funding: This research is partly supported by the National Natural Science Foundation of China (Grant No. 52202391, 52302510, and U20A20155) and the Fundamental Research Funds for the Central Universities (Grant No.YWF-23-Q-1066).

Data Availability Statement: Our data will be available at https://github.com/LongboCheng123/Electronics-2623630-dataset.git.

Conflicts of Interest: The authors declare no conflict of interest.

References

1. Li, Y.; Wang, F.; Fan, G.; Liu, Y.; Zhang, Y. A Fast Estimation Algorithm for Parameters of Multiple Frequency-Hopping Signals Based on Compressed Spectrum Sensing and Maximum Likelihood. *Electronics* **2023**, *12*, 1808. [CrossRef]
2. Liu, X.; Guan, M.; Zhang, X.; Ding, H. Spectrum Sensing Optimization in an UAV-Based Cognitive Radio. *IEEE Access* **2018**, *6*, 44002–44009. [CrossRef]
3. Luo, Z.; Wang, X. A High-efficiency Collaborative Spectrum Sensing with Gated Recurrent Unit for Multi-UAV Network. In Proceedings of the 31st International Telecommunication Networks and Applications Conference (ITNAC), University of New South Wales, Sydney, Australia, 24–16 November 2021; pp. 180–187.
4. Abdel-Rahman, M.J.; Krunz, M. Game-theoretic quorum-based frequency hopping for anti-jamming rendezvous in DSA networks. In Proceedings of the 2014 IEEE International Symposium on Dynamic Spectrum Access Networks (DYSPAN), McLean, VA, USA, 1–4 April 2014; pp. 248–258. [CrossRef]
5. Si, P.; Yu, F.R.; Yang, R.; Zhang, Y. Dynamic Spectrum Management for Heterogeneous UAV Networks with Navigation Data Assistance. In Proceedings of the IEEE Wireless Communications and Networking Conference (WCNC), New Orleans, LA, USA, 9–12 March 2015; pp. 1078–1083.
6. Jia, L.; Xu, Y.; Sun, Y.; Feng, S.; Yu, L.; Anpalagan, A. A Game-Theoretic Learning Approach for Anti-Jamming Dynamic Spectrum Access in Dense Wireless Networks. *IEEE Trans. Veh. Technol.* **2019**, *68*, 1646–1656. [CrossRef]
7. Lee, C.; Jang, G.; Dao, N.N.; Lakew, D.S.; Lee, C.; Cho, S. Competitive Game Theoretic Clustering-Based Multiple UAV-Assisted NB-IoT Systems. *Electronics* **2021**, *10*, 356. [CrossRef]
8. Charlesworth, P.B. A Non-cooperative Game to Coordinate the Coverage of two Communications UAVs. In Proceedings of the IEEE Military Communications Conference, BAE Syst, San Diego, CA, USA, 18–20 November 2013; pp. 668–673.
9. Chen, X.C.; Chen, Y.J. A Machine Learning Based Attack in UAV Communication Networks. In Proceedings of the 2019 IEEE 90th Vehicular Technology Conference (VTC2019-Fall), Honolulu, HI, USA, 22–25 September 2019; pp. 1–2. [CrossRef]
10. Chang, Z.; Guo, W.; Guo, X.; Ristaniemi, T. Machine Learning-based Resource Allocation for Multi-UAV Communications System. In Proceedings of the 2020 IEEE International Conference on Communications Workshops (ICC WORKSHOPS), Dublin, Ireland, 7–11 June 2020.
11. Du, F.; Li, J.; Lin, Y.; Wang, Z.; Qian, Y. Mean-Field Multi-Agent Reinforcement Learning for Adaptive Anti-Jamming Channel Selection in UAV Communications. In Proceedings of the 14th IEEE International Conference on Wireless Communications and Signal Processing (WCSP), Nanjing, China, 1–3 November 2022; pp. 910–915.
12. Gao, Y.; Xiao, Y.; Wu, M.; Xiao, M.; Shao, J. Game Theory-Based Anti-Jamming Strategies for Frequency Hopping Wireless Communications. *IEEE Trans. Wirel. Commun.* **2018**, *17*, 5314–5326. [CrossRef]
13. Du, J.; Tian, W.; Ji, X.; Du, M.; Liu, G.; Dai, Y.; Han, Z. Strategic UAV-Assisted Game Model for Detection in Covert Communication. *IEEE Trans. Veh. Technol.* **2023**, *72*, 7426–7438. [CrossRef]
14. Jose, S.T.; Kulkarni, A.A. Shannon Meets von Neumann: A Minimax Theorem for Channel Coding in the Presence of a Jammer. *IEEE Trans. Inf. Theory* **2020**, *66*, 2842–2859. [CrossRef]
15. Yu, J.; Li, Q. Optimal Deployment in Moving Target Defense against Coordinated Cyber-Physical Attacks via Game Theory. *Electronics* **2023**, *12*, 2484. [CrossRef]
16. Wu, Y.; Wang, B.; Liu, K.J.R.; Clancy, T.C. Anti-Jamming Games in Multi-Channel Cognitive Radio Networks. *IEEE J. Sel. Areas Commun.* **2012**, *30*, 4–15. [CrossRef]

17. Ruan, L.; Wang, J.; Chen, J.; Xu, Y.; Yang, Y.; Jiang, H.; Zhang, Y.; Xu, Y. Energy-Efficient Multi-UAV Coverage Deployment in UAV Networks: A Game-Theoretic Framework. *China Commun.* **2018**, *15*, 194–209. [CrossRef]
18. Li, H.; Han, Z. Blind Dogfight in Spectrum: Combating Primary User Emulation Attacks in Cognitive Radio Systems with Unknown Channel Statistics. In Proceedings of the 2010 IEEE International Conference on Communications, Cape Town, South Africa, 23–27 May 2010; pp. 1–6. [CrossRef]
19. Lei, Z.; Yang, P.; Zheng, L. Detection and Frequency Estimation of Frequency Hopping Spread Spectrum Signals Based on Channelized Modulated Wideband Converters. *Electronics* **2018**, *7*, 170. [CrossRef]
20. Xu, Y.; Ren, G.; Chen, J.; Zhang, X.; Jia, L.; Kong, L. Interference-Aware Cooperative Anti-Jamming Distributed Channel Selection in UAV Communication Networks. *Appl. Sci.* **2018**, *8*, 1911. [CrossRef]
21. Jia, L.; Yao, F.; Sun, Y.; Niu, Y.; Zhu, Y. Bayesian Stackelberg Game for Antijamming Transmission with Incomplete Information. *IEEE Commun. Lett.* **2016**, *20*, 1991–1994. [CrossRef]
22. Garnaev, A.; Petropulu, A.; Trappe, W.; Poor, H.V. A Multi-Jammer Power Control Game. *IEEE Commun. Lett.* **2021**, *25*, 3031–3035. [CrossRef]
23. Feng, Z.; Ren, G.; Chen, J.; Zhang, X.; Luo, Y.; Wang, M.; Xu, Y. Power Control in Relay-Assisted Anti-Jamming Systems: A Bayesian Three-Layer Stackelberg Game Approach. *IEEE Access* **2019**, *7*, 14623–14636. [CrossRef]
24. Qi, N.; Wang, W.; Zhou, F.; Jia, L.; Wu, Q.; Jin, S.; Xiao, M. Two Birds with One Stone: Simultaneous Jamming and Eavesdropping with the Bayesian-Stackelberg Game. *IEEE Trans. Commun.* **2021**, *69*, 8013–8027. [CrossRef]
25. Su, Z.; Wu, Q.; Qi, N.; Jia, L.; Du, Z. Biased Stackelberg game-based UAV relay anti-jamming communications: Exploiting trajectory optimization and transmission mode selection. *IET Commun.* **2022**, *16*, 2467–2478. [CrossRef]
26. Xie, L.; Su, Z.; Chen, N.; Xu, Q.; Fan, Y.; Benslimane, A. A Game Theory Based Scheme for Secure and Cooperative UAV Communication. In Proceedings of the ICC 2021—IEEE International Conference on Communications, Montreal, QC, Canada, 14–23 June 2021.
27. Han, C.; Huo, L.; Tong, X.; Wang, H.; Liu, X. Spatial Anti-Jamming Scheme for Internet of Satellites Based on the Deep Reinforcement Learning and Stackelberg Game. *IEEE Trans. Veh. Technol.* **2020**, *69*, 5331–5342. [CrossRef]
28. Xu, Y.; Ren, G.; Chen, J.; Jia, L.; Xu, Y. Anti-jamming transmission in UAV communication networks: A Stackelberg game approach. In Proceedings of the 2017 IEEE/CIC International Conference on Communications in China (ICCC), Qingdao, China, 22–24 October 2017. [CrossRef]
29. Xu, J.; Wang, K.; Zhang, X.; Liu, P.; Kong, D.; Zhou, H. Anti-jamming strategy based on game theory in single-channel UAV communication network. In Proceedings of the 2021 Sixth International Conference on Fog and Mobile Edge Computing (FMEC), Gandia, Spain, 6–9 December 2021; pp. 63–69.
30. Liao, C.; Xu, K.; Zhu, H.; Xia, X.; Su, Q.; Sha, N. Secure transmission in satellite-UAV integrated system against eavesdropping and jamming: A two-level stackelberg game model. *China Commun.* **2022**, *19*, 53–66. [CrossRef]
31. Zhu, X.; Huang, Y.; Wang, S.; Wu, Q.; Ge, X.; Liu, Y.; Gao, Z. Dynamic Spectrum Anti-Jamming with Reinforcement Learning Based on Value Function Approximation. *IEEE Wirel. Commun. Lett.* **2023**, *12*, 386–390. [CrossRef]
32. Zou, M.; Chen, J.; Luo, J.; Hu, Z.; Chen, S. Equilibrium Approximating and Online Learning for Anti-Jamming Game of Satellite Communication Power Allocation. *Electronics* **2022**, *11*, 3526. [CrossRef]
33. Hashesh, A.O.; Hashima, S.; Zaki, R.M.; Fouda, M.M.; Hatano, K.; Eldien, A.S.T. AI-Enabled UAV Communications: Challenges and Future Directions. *IEEE Access* **2022**, *10*, 92048–92066. [CrossRef]
34. Li, Y.; Xu, Y.; Xu, Y.; Liu, X.; Wang, X.; Li, W.; Anpalagan, A. Dynamic Spectrum Anti-Jamming in Broadband Communications: A Hierarchical Deep Reinforcement Learning Approach. *IEEE Wirel. Commun. Lett.* **2020**, *9*, 1616–1619. [CrossRef]
35. Wu, Q.; Wang, H.; Li, X.; Zhang, B.; Peng, J. Reinforcement Learning-Based Anti-Jamming in Networked UAV Radar Systems. *Appl. Sci.* **2019**, *9*, 5173. [CrossRef]
36. Von Neumann, J. Zur Theorie der Gesellschaftsspiele. *Math. Ann.* **1928**, *100*, 295–320. [CrossRef]
37. Vajda, S. Games and Decisions. By R. Duncan Luce and Howard Raiffa. Pp. xi, 509. 70s. 1957. (J Wiley & Sons). *Math. Gaz.* **1959**, *43*, 152–153.

Disclaimer/Publisher's Note: The statements, opinions and data contained in all publications are solely those of the individual author(s) and contributor(s) and not of MDPI and/or the editor(s). MDPI and/or the editor(s) disclaim responsibility for any injury to people or property resulting from any ideas, methods, instructions or products referred to in the content.